ISSN: 0975-833X

*Available online at http://www.journalcra.com*

*International Journal of Current Research*
*Vol. 18, Issue, 04, pp.36922-36928, April, 2026*
*DOI: https://doi.org/10.24941/ijcr.50495.04.2026*

**INTERNATIONAL JOURNAL OF CURRENT RESEARCH**

# RESEARCH ARTICLE

## SYNTHESIS, SOLVATOCHROMIC TUNING, AND CHARGE TRANSPORT PROPERTIES OF BIMETALLIC ($M_2$(DPBD)$(OAC)_2$) (M = CU, NI, & ZN) COMPLEXES: A STUDY OF MAGNETIC HARDNESS AND SEMICONDUCTING BEHAVIOR

**Venkatesh Gaddameedi, Venkateshwarlu Rao D., Ranjith Kore and Someshwar Pola***

Department of Chemistry, Osmania University, Hyderabad, Telangana, India

**ARTICLE INFO**

*Article History:*
Received 14th January, 2026
Received in revised form
24th February, 2026
Accepted 25th March, 2026
Published online 30th April, 2026

*Key Words:*
Bimetallic Systems, Chelation-Enhanced Fluorescence, Optoelectronic.

**Corresponding author:*
**Venkatesh Gaddameedi**

**ABSTRACT**

In this research, we report the synthesis and complete characterization of multiple bimetallic complexes that were based on the ligand 2,5-bis(pyridin-2-yl)benzene-1,4-diol (DPBD). The complexes ($M_2$(DPBD)$(OAc)_2$) (M = Cu(II), Ni(II), &Zn(II)) were prepared using an easy reflux process and analyzed by methods of UV-Vis, Photoluminescence (PL), and Thermogravimetric Analysis (TGA). Major ligand-to-metal charge transfer (LMCT) transitions and a small reduction of the optical band gap (Eg) from 3.48 eV in the free ligand to as low as 2.63 eV in the complexes were shown by UV-Vis spectroscopy. The photoluminescence studies showed a coordination-induced blue shift and suppression of Excited-State Intramolecular Proton Transfer (ESIPT), with the Zn (II) complex showing Chelation-Enhanced Fluorescence (CHEF) in protic media. VSM-based magnetic studies at 300 K demonstrated that ($Ni_2$(DPBD)) was a magnetically harder material than ($Cu_2$(DPBD)), displaying increased saturation magnetization (3.14 B.M.) and coercivity. In addition, AC conductivity and dielectric analyses verify the semi-conductivity of the frameworks, where ($Cu_2$(DPBD)) has the highest conductivity (75 x $10^{-4}$ $\Omega^{-1}m^{-1}$). Nyquist plots (temperature dependent) showed a thermally activated hopping mechanism with systematic resistance reduction; these bimetallic systems exhibit potential for both optoelectronic and temperature-sensing applications.



**Citation: Venkatesh Gaddameedi, Venkateshwarlu Rao D., Ranjith Kore and Someshwar Pola. 2026.** "Synthesis, solvatochromic tuning, and charge transport properties of bimetallic (m2(dpbd)(oac)2) (m = cu, ni, & zn) complexes: a study of magnetic hardness and semiconducting behavior*". International Journal of Current Research*, 18 (04), 36922-36928.

# INTRODUCTION

The development and construction of functional coordination complexes have become a fundamental element in contemporary materials science, owing to the research focus on the development of molecular-scale electronic and magnetic devices (1-3). Among different architectural forms, bimetallic or binuclear complexes are interesting, because of their synergistic properties when interacting with one another through the lens of a bridging organic framework (4). These interactions could typically give rise to physical properties, such as long-range magnetic ordering, increased charge transfer and tunable photophysical properties, that are radically different from their mononuclear counterparts (5). One challenge in this work is the choice of a ligand structure with an electronic communication pathway that bridges two metal centers. In this sense, heterocyclic ligands containing both nitrogen and oxygen donor atoms are particularly successful (6,7). We present a complex structural scaffold for these purposes as the ligand 2,5-bis(pyridin-2-yl)benzene-1,4-diol (DPBD). DPBD consists of a central hydroquinone moiety which is surrounded by a pair of pyridine rings, thus establishing a symmetric tetradentate (N2,O2) coordination environment. Such setup enables stabilization of binuclear (M2) clusters at which the metal ions are bridged by the phenolate oxygens of the central ring. DPBD not only possesses structural feasibility; it belongs to the class of molecules for Excited-State Intramolecular Proton Transfer (ESIPT) (8). In untethered state, the hydroxyl protons' close proximity to the pyridine nitrogen's leads to fast tautomerization (when photoexcited) that results in a large Stokes-shifted green emission (9). The metal ions, on the other hand, substitute such intramolecular hydrogen bonds with rigid metal-ligand coordinate bonds (10). This "locking" of the molecular framework also inhibits ESIPT and also triggers Chelation-Enhanced Fluorescence (CHEF) and Ligand-to-Metal Charge Transfer (LMCT) processes that can drastically reduce the optical band gap (11). They also allow manipulation of magnetic and electrical transport properties when transition metals (such as Cu(II), Ni(II), and Zn(II)) are integrated into the DPBD model. Cu(II) (d9) and Ni(II) (d8) centers provide unpaired electrons in the system and allow investigation into magnetic exchange and anisotropy (12). With recent advances in magnetic hardness and coercivity to molecular system, these bimetallic clusters are prospective candidates for molecular

magnetic memory (13). At the same time, the semiconducting character of these coordination polymers also, frequently a result of hopping mechanisms or quantum mechanical tunnelling, can provide an opportunity for organic-inorganic hybrid semiconductors (14,15). Here, we report the preparation and detailed characterization of a series of bimetallic (M2(DPBD)$(OAc)_2$) complexes (M = Cu, Ni, & Zn). Our methodologies are cross-disciplinary to determine their properties: UV-Vis and Photoluminescence spectroscopies for their solvatochromic tuning and band-gap narrowing effect; Thermogravimetric Analysis (TGA) to demonstrate the thermal stability of the binuclear bonding; and Vibrating Sample Magnetometry (VSM) to compare the magnetic hardness of the Cu and Ni precursors. Overall, we investigate the AC conductivity and temperature-dependent impedance characteristics for understanding the charge transport mechanisms in these frameworks. There is a major importance of this study to guide us on how metal centre, and solvent environment, can adapt the specific multi-functional performance of DPBD-based bimetallic materials.

**Experimental Section**

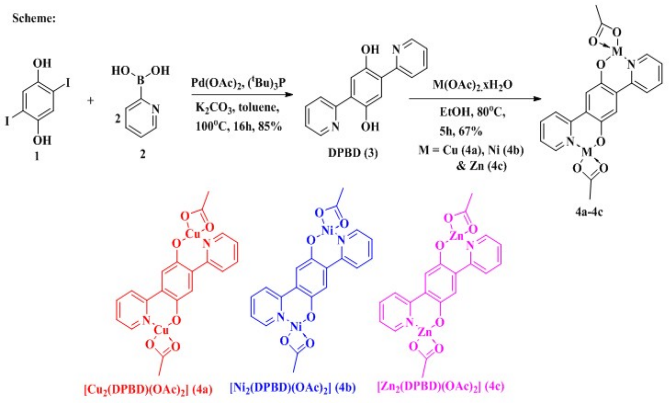


# METHODS AND MATERIALS

All reagents and solvents were purchased from commercial suppliers and used without further purification unless otherwise noted. Toluene was distilled over sodium/benzophenone under a nitrogen atmosphere. 2,5-diiodobenzene-1,4-diol (**1**) and pyridin-2-ylboronic acid (**2**) were obtained from Sigma-Aldrich. $^{1}H$ and $^{13}C$ NMR spectra were recorded on a Bruker 400 MHz spectrometer. Elemental analyses were performed on a UnicubeOrganic elemental analyzer.

**Synthesis of 2,5-di(pyridin-2-yl)benzene-1,4-diol (DPBD, 3)** In a 100 mL two-neck round-bottom flask equipped with a reflux condenser and a magnetic stir bar, 2,5-diiodobenzene-1,4-diol (**1**) (1.0 mmol), pyridin-2-ylboronic acid (**2**) (2.5 mmol), and anhydrous $K_2CO_3$ (4.0 mmol) were suspended in dry toluene (30 mL). The mixture was degassed by three freeze-pump-thaw cycles or by bubbling nitrogen for 20 minutes. Subsequently, $Pd(OAc)_2$ (0.05 mmol) and $P(^tBu)_3$ (0.10 mmol) were added under a nitrogen atmosphere.The reaction mixture was heated at 100°C with vigorous stirring for 16 hours. After cooling to room temperature, the mixture was diluted with dichloromethane (50 mL) and washed with water (3 x 30 mL) and brine. The organic layer was dried over anhydrous $Na_2SO_4$, filtered, and concentrated under reduced pressure. The crude residue was purified by silica gel column chromatography using a mixture of solvent system, (EtOAc:MeOH (9.5:0.5)) to afford DPBD (3) as a yellow solid.Yield: 85%

**General Procedure for the Synthesis of Binuclear Complexes ($M_2$(DPBD)$(OAc)_2$) (4a-4c):** To a solution of **DPBD (3)** (0.2 mmol) in absolute ethanol (15 mL), the appropriate metal acetate hydrate $M(OAc)_2.xH_2O$ (0.44 mmol, 2.2 equiv.) was added. The reaction mixture was heated to 80°C and stirred for 5 hours. During this time, a colored precipitate formed. The mixture was cooled to room temperature, and the precipitate was collected by vacuum filtration. The solid was washed thoroughly with cold ethanol and diethyl ether, and then dried under vacuum to get 67% of respective complexes.

# RESULTS AND DISCUSSION

***UV-Vis Absorption Spectroscopic Analysis of DPBD and its Metal Complexes:*** Electronic absorption spectra of ligand 2,5-bis(pyridin-2-yl)benzene-1,4-diol (DPBD) and its binuclear complexes with Cu(II), Ni(II), and Zn(II) acetates were studied in four solvents varying in polarity and coordinating ability: DMF, THF, MeOH, and DMSO. The proposed work seeks to elucidate how solvent-solute interaction and metal coordination impact the electronic structure and optical characteristics of the DPBD system. As the free ligand DPBD shows characteristic absorption bands in the UV region that include band-I (~240 nm), this is attributed to the high-energy π→π* transitions of the aromatic rings (pyridine and hydroquinone). Band-II (~285–296 nm) corresponds to the π→π* transitions in the conjugated system. Band III (~325–330 nm) is associated with n→π* transitions involving the lone pairs on the nitrogen atoms of the pyridine rings and oxygen atoms of the hydroxyl groups.

The ligand has a specific sensitivity to the solvent environment. In THF (red line), the absorbance is much higher than DMSO or MeOH, and fine structure is more significant. The optical band gap ($E_g$) for the ligand is relatively stable among solvents, ranging from 3.45 eV to 3.49 eV, implying solvent polarity affects the probability that transition will occur (intensity), although the energy gap between the primary transitions is still mainly intrinsic to the molecular structure. Following coordination with Cu(II), Ni(II), and Zn(II) ions, changes in the spectra are observed in all solvents, as detailed in Figures 1b) through 1e, along with new, broad absorption bands in the 350–450 nm region. In DMF (Figure 1b), an intense red shift appears in the complexes. As an example, the ($Cu_2$(DPBD)) complex has a peak at 366 nm and the ($Ni_2$(DPBD)) complex at 392 nm. The change is consistent with ligand-to-metal charge transfer (LMCT) transitions of the phenolate oxygen or pyridine nitrogen to the metal d-orbitals. The disappearance of the n→π* band of the free ligand near 330 nm indicates the role of heteroatoms in coordination.

By coordination, the optical band gap gets dramatically narrowed, e.g. ($Cu_2$(DPBD)) ($E_g$) = 2.63 - 2.83 eV (Strongest reduction), ($Ni_2$(DPBD)) ($E_g$) = 2.65 - 2.88 eV. ($Zn_2$(DPBD)) ($E_g$) in the range of 2.63 - 2.95 eV. The decreased $E_g$ (from 3.48 eV (in the ligand) to 2.63 eV (in the complexes)) demonstrates higher activation strength and electronic delocalization across this metal-ligand circuit. In MeOH (Figure 1c), and THF (Figure 1d), the complexes have strong

UV bands (200–300 nm), but LMCT bands are less intense compared to those of DMF/DMSO. This indicates the electronic transitions, in less coordinated solvents, are dominated by the internal π→π* structure of the ligand. In DMF (Figure 1b) and DMSO (Figure 1e), the bands are complex and larger and intensity. The ($Cu_2$(DPBD)) complex (red line) in DMSO (Figure 1e) has an unmistakable peak at 394 nm. The ($Ni_2$(DPBD)) complex (blue line) shows a maximum at 392 nm in DMF (Figure 1b). DMF/DMSO's high polarity and coordinating quality are expected to stabilize the charge-separated states (LMCTs) and promote such transitions. For Cu (II) (Red), the lowest Eg values for most solvents are usually observed (2.63 eV in DMF), indicating that the Cu(II) center is a candidate that can overlap efficiently with the electronic transitions. Ni (II) (Blue), demonstrated stable LMCT bands at a range of 385–400 nm. In d10 Zn (II) (Pink), the transitions in Zn complex are mostly ligand-centred or LMCT, usually approximating the features of ligand but shifted, Eg values commonly greater than Cu(II) but less than free ligand. Consequently, the ultraviolet-visible study results indicate an efficient synthesis of binuclear-metal complexes confirmed by a striking red-shift of absorption maxima in addition to an optical band gap closure. The solvatochromic analysis suggests that, although the ligand is relatively stable, metal complexes are strongly soluble in polar aprotic solvents, such as DMF and DMSO, promoting charge transfer. These properties are indicative of their possible use as optoelectronic molecules, or also as sensors for specific solvent applications.

***Photoluminescence (PL) Spectroscopic Analysis of DPBD and its Metal Complexes:*** The photoluminescence properties of 2,5-bis(pyridin-2-yl)benzene-1,4-diol (DPBD) were investigated in solvents having different polarity (THF, MeOH, DMF, DMSO). The free ligand can be viewed from Figure 2a, and an emission band around a wavelength of approximately 483 nm to 500 nm is observed. λem changes from 483 nm in THF (least polar) to 500 nm in MeOH, and 497 nm in DMF/DMSO. This bathochromic shift with increasing solvent polarity indicates a π→π* transition in a more polar excited state (positive solvatochromism). The quantum yield order of the emission intensity is highest in THF (red curve), which means, the non-polar environment has minimized nonradiative relaxation pathways but due to the increased polar protic solvents like MeOH or strongly polar aprotic solvents like DMF partial quenching. Coordination with Cu(II), Ni(II), and Zn(II) results in markedly different emission spectra that are characterized by blue-shifted emission bands and modulation of intensity. Concerning significant Hypsochromic Shifts (Blue Shifts) compared to ligand at 490 nm, the complexes show sharper emissions in the 350–450 nm range, but Cu (II) and Ni (II) complexes are seen to exhibit sharp peaks of 380–410 nm across a variety of solvents. Zn (II) complexes, on the contrary, tend to display a dual emission or a considerably blue-shifted peak (at 451 nm in DMF, 393 nm in THF). The blue shift is probably the result of coordinating and stabilization of ligand's ground state or the suppression of the Excited-State Intramolecular Proton Transfer (ESIPT) process. As DPBD's hydroxyl groups ortho to pyridine nitrogen's is used in order to achieve coordination, coordination then replaces the internal hydrogen bond in the molecule with a metal-ligand one to lock it and shift emission manifold. Ni(II) (blue) and Cu(II) (red) complexes show very narrow and intense emission at 402 nm and 407 nm for the crystal structures of DMF (Figure 2b). The peak of the Zn(II) complex (pink) is wider at 451 nm. Remarkably, the broad ligand-centered emission at 494 nm is very suppressive in the Cu and Ni complexes, although shoulders are present in the Zn complex. Meanwhile, the Cu(II) and Ni(II) complexes in methanol (Figure 2c) exhibit almost the same sharp peaks at 394 nm and 398 nm. The Zn(II) complex (pink) shows much increase at 475 nm, indicative of aggregation emission induced (AIE), or that of formation of highly fluorescent Zn-chelate species, which effectively avoided non-radiative decay in the protic environment. In contrast, at 379 nm, the Ni(II) complex (blue) in THF is highly emissive (Figure 2d). The Zn(II) complex exhibits two discrete areas including a well-defined peak at 393 nm and a broad shoulder at 463 nm. Whereas, in the free ligand (black) it is maintained as the dominant one at 484 nm, suggested that in THF the coordination equilibrium might have a more favored ligand's native state than it does in DMF. In addition, DMSO (Figure 2e), in the Cu(II) complex shows a strong peak at 349 nm. It can be observed at 427 nm for the Ni(II) complex. Refined Zn(II) complex emits at 404 nm and 487 nm respectively. It was realized that DMSO's strong coordinating ability affects the coordination sphere of the metal, thereby modifying the energy in the complexes. Cu (II) and Ni (II) complexes are paramagnetic ions such as Cu (II) ($d^9$) and Ni (II) ($d^8$) that quench the fluorescence through electron transfer, energy transfer or similar phenomena. In this system however, we find new, extremely high-energy sharp bands arising.

This indicates that the coordination imposes a novel, stiffened emissive state (Chelation-Enhanced Fluorescence, CHEF) at a higher energy level, albeit with slightly lower overall intensity compared to the free ligand in THF. Zn (II) complex is $d^{10}$ ionized, Zinc helps to improve fluorescence, making the ligand more rigid and inhibiting internal rotations. Particularly in contrast to other species, Methanol Figure 2c reveals that the Zn-complex intensity is strikingly high. The PL data shows a more elaborate interaction between metal coordination, which has a complex interaction with the solvent effects while coordination probably suppresses the ESIPT mechanism of the DPBD ligand, shifting emission from the green area (□500 nm) to UV-blue area (~380-420 nm). The emission wavelength and intensity are tightly dependent on the choice of solvent, where methanol shows favouritism towards fluorescence from Zn and DMF/DMSO provides sharp UV-blue peaks for Cu (II) and Ni (II) complexes. The broad emission band of the ligand disappears in solution and also new metal-specific peaks appear so the binuclear complexes formed in solution are confirmed.

***Thermogravimetric Analysis (TGA) of DPBD and its Binuclear Metal Complexes:*** The TGA thermogram of the free ligand 2,5-bis(pyridin-2-yl)benzene-1,4-diol (DPBD), represented by the black curve, shows a single, rapid weight loss step starting at approximately 310 °C and concluding around 410 °C as shown in Figure 3. It indicates that the ligand undergoes complete decomposition/volatilization, leaving almost zero residue (near 0% remaining weight) by 450 °C. Therefore, high purity of the organic ligand and a lack of any non-volatile components. The presence of specific complexes ($Cu_2$(DPBD)$(OAc)_2$) (red), ($Ni_2$(DPBD)$(OAc)_2$) (blue), and ($Zn_2$(DPBD)$(OAc)_2$) (pink) is observed in this paper, in contrast to the ligand, as the decomposition method of the complexes indicates a more sophisticated structural assembly. The first mass loss is at 150–320 °C for (Cu (II) complex 23.39%, Ni (II) complex 23.81%, and Zn (II) complex 23.26%).

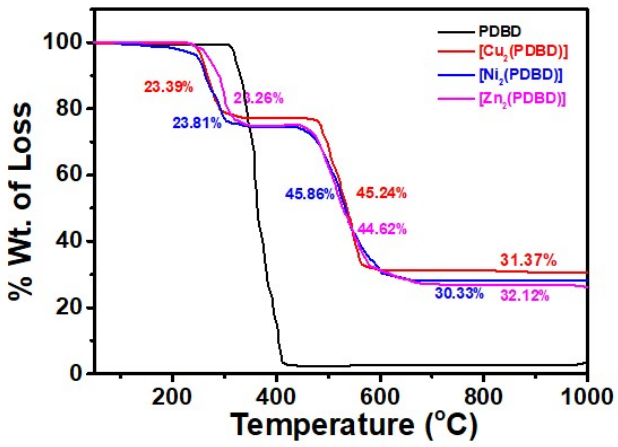


**Figure 3. Thermograms of ligand DPBD, ($Cu_2$(DPBD)), ($Ni_2$(DPBD)), and ($Zn_2$(DPBD)) complexes**

This stage is due to the decay of coordinated acetate (-OAc) groups and possibly any very tightly bound lattice or coordinated molecules (such as water or MeOH that are employed in synthesis). Weight loss is similar across the three complexes (around 23%), meaning that the stoichiometry in the coordination domain is common to all. Although stage-2 degradation does have a temporary plateau in stability, a second major reduction in weight (as shown in Figure 3) followed (450 °C - 650 °C). (Cu (II) complex: 45.24 percent; Ni (II) complex: 45.86 percent; Zn (II) complex: 44.62 percent). This showed that the DPBD ligand backbone is being oxidatively thermally degraded. Given that this step takes place at a much higher temperature than the decomposition of the free ligand (which ends at 410 °C), its coordination to metal ions greatly ensures the thermal stability of the organic framework. The complexes reach a constant plateau above 700 °C. That's the remaining weight that indicates the formation of stable metal oxides (CuO, NiO, and ZnO). The Cu (II) complex residue is 31.37% (consistent with CuO residue), and the Ni (II) complex residue is 30.33% (consistent with NiO residue). Zn (II) complex residue remains; 32.12% (corresponding to ZnO residue). The complexes start losing weight faster than that of ligands (150 °C vs 310 °C) as volatile acetate/solvents are removed. However, the core ligand-metal structure remains present until 450 °C, and the free ligand disappears entirely by 410 °C. The thermal stability profiles for each of the metals are remarkably consistent, indicating the structural rigidity is driven more by the binuclear bridging mode of the DPBD ligand than by the specificity of the divalent metal cation. Thus, the TGA results confirm the formation of the binuclear complexes. The weight loss percentage for the first step (~23%) and the second step (~45%) are consistent with the stoichiometry obtained in the experiment between two metal ions and two acetate groups per ligand unit. High % residual metal oxides at 1000 °C also confirms metal loading of the complexes, serving as a quantitative approximation to the structural formulas suggested in our present study.

***Analysis of Magnetic Properties for ($Cu_2$(DPBD)) and ($Ni_2$(DPBD)):*** The magnetic characteristics of bimetallic complexes ($Cu_2$(DPBD)) and ($Ni_2$(DPBD)) were analyzed by Vibrating Sample Magnetometry (VSM) at room temperature as depicted in Figure 4. The measurements were performed on samples with the masses ($Cu_2$(DPBD)) (Red): 12.8 mg and ($Ni_2$(DPBD)) (Blue): 13.6 mg, and the magnetic moment (M) was expressed as a function of the applied magnetic field (H) between –20,000 and +20,000 Oe.

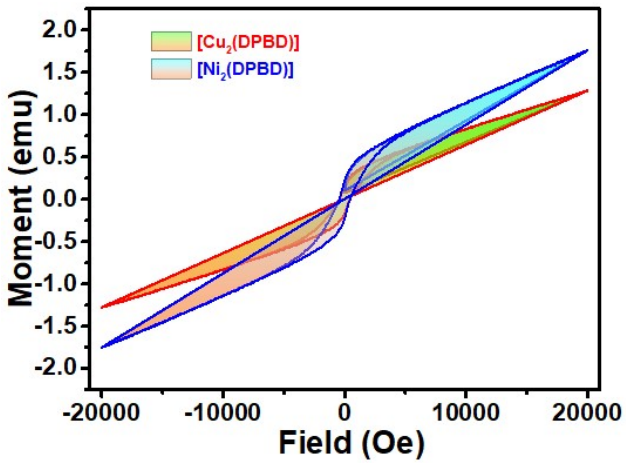


**Figure 4 Room temperature (300 K) field-dependent magnetization (M vs H) curves for bimetallic complexes ($Cu_2$(DPBD)) (red) and ($Ni_2$(DPBD)) (blue). The plots illustrate the variation in magnetic moment (emu) within an applied magnetic field range of -20,000 to +20,000 Oe**

($Ni_2$(DPBD)) (Blue Curve) has a high magnetic moment where the maximum field (20,000 Oe) is around 1.75 emu (3.14 B.M). Since the curve slope is steeper than the Copper analog, it shows relatively high magnetic susceptibility. ($Cu_2$(DPBD)) (Red Curve) shows a lower magnetic moment of approximately 1.25 emu (1.68 B.M.) at 20,000 Oe.

***Hysteresis and Coercivity:*** Both complexes show characteristic hysteresis loops, indicating a certain ferromagnetic or ferrimagnetic behavior at room temperature. Compared with ($Cu_2$(DPBD)), the hysteresis loop (the area) of the ($Ni_2$(DPBD)) complex is significantly wider. This indicates significantly greater magnetic remanence (Mr) and coercivity (Hc), which suggests that the Nickel-based complex has "harder" magnetic properties compared to the Copper-based complex. The "waisted" or constricted shape of the loops around the origin indicates possible complex magnetic processes (potentially domain wall pinning or some combination of magnetic phases/anisotropies within the bimetallic framework). The result of VSM clearly shows that the magnetic response depending on the metal center in the DPBD framework is significant. The slightly higher observed moment for ($Ni_2$(DPBD)) is in agreement with Ni(II) (d8) electronic configuration as compared with Cu(II) (d9). In octahedral or pseudo-octahedral schemes, Ni(II) generally has 2 unpaired electrons per metal center (S=1) and Cu(II) has 1 (S=1/2). In conclusion, this suggests that the cumulative spin density of (Ni2(DPBD)) system is theoretically higher and in agreement with experimental M vs H data. Overall, the broader loop of the ($Ni_2$(DPBD)) indicates a higher magneto-crystalline anisotropy. Ni(II) ions have considerable Zero-Field Splitting (ZFS) and anisotropy when compared to the more isotropic Cu(II) ions. This anisotropy prevents an easy reversal of the magnetic moment, causing an increase in coercivity observed. The shape of these loops, especially the non-linear behavior at low fields, indicates the DPBD ligand serves for the magnetic exchange between the two metal centers. The presence of a clear hysteresis loop at room temperature is surprising, especially for such molecular complexes, confirming high magnetic ordering or slow

relaxation of magnetization during bulk formation. Therefore, ($Ni_2$(DPBD)) presented better magnetic behavior under the comparison of total moment and coercivity with ($Cu_2$(DPBD)). These results indicate that the selected metal ion is important to modulate both the magnetic hardness and saturation of DPBD-based bimetallic systems, and the Nickel type is a better candidate if magnetization memory or susceptibility is a concern.

***Comparative AC Conductivity and Impedance Analysis of ($M_2$(DPBD)) Complexes AC Conductivity ($\sigma_{ac}$) Profiling:*** The frequency sensitive AC conductivity (σac) for the (Cu2(DPBD)), (Ni2(DPBD)), and (Zn2(DPBD)) complexes were observed for $10^2$–$10^6$ Hz. Frequency-dependent behavior of disordered semiconducting materials is found for all three complexes. In all three instances, the conductivity is fairly constant in low frequency (DC-like plateau) and increases dramatically in high frequency. This behavior follows Jonscher's Universal Power Law:

$$\sigma_{total}(\omega) = \sigma_{dc} + A\omega^s$$

Where:

$\sigma_{dc}$ is the frequency-independent conductivity; A is a temperature-dependent parameter; and s is the power-law exponent ($0 < s < 1$), representing the degree of interaction between mobile ions/carriers and the lattice. ($Cu_2$(DPBD)) (Figure 6a), as it showed the highest conductivity at 75 x $10^{-4}$ $\Omega^{-1}m^{-1}$ at $10^6$ Hz. The high steep increase at high frequencies indicates good hopping-type conduction, as observed in Fig. ($Ni_2$(DPBD)) (Figure 6b), exhibited marginally reduced conductivity for comparison to the Copper analogue reaching the maximum values of 65 x $10^{-4}$ $\Omega^{-1}m^{-1}$. ($Zn_2$(DPBD)) (Figure 6c), which was found to have the lowest relative conductivity, and also to attain 40 x $10^{-4}$ $\Omega^{-1}m^{-1}$. In contrast to Cu and Ni analogues that have a rapid increase at high frequencies, the Zn complex exhibits a less abrupt (almost linear) rise in log scale at high frequencies, indicating a different distribution of relaxation times or a more limited hopping mechanism.

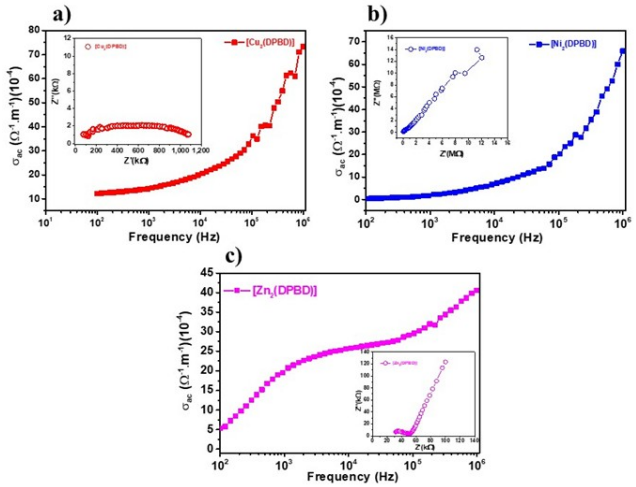


**Figure 5. Frequency dependence of AC conductivity ($\sigma_{ac}$) and corresponding Nyquist plot insets for bimetallic complexes: a) ($Cu_2$(DPBD)), b) ($Ni_2$(DPBD)), and c) ($Zn_2$(DPBD)). The main panels illustrate the variation of $\sigma_{ac}$ from $10^2$ to $10^6$ Hz, showcasing the universal power-law behavior and thermally activated hopping mechanisms. The insets show the complex impedance plots (-Z'' vs. Z'), providing a comparative visualization of the bulk resistance ($R_b$) and charge-transfer characteristics for each metal-organic system**

The insets provide crucial information about the bulk resistance ($R_b$) and charge transfer mechanisms of the materials. In the complex inset, a clear semicircular arc observed in ($Cu_2$(DPBD)) complex with a diameter ($R_b$) of approximately 1,100 kΩ was obtained. This relatively low resistance (compared to the Ni analog) explains its superior AC conductivity. ($Cu_2$(DPBD)) complex inset shows an incomplete large semicircular arc extending into the MΩ range (12 MΩ). This suggests a drastically larger bulk resistance, which is consistent with the lower $\sigma_{ac}$ in the corresponding main plot. At high frequencies, ($Zn_2$(DPBD)) complex inset exhibited a small semicircle, followed by a Warburg-type upward tail at lower frequencies (right edge of arc). Such tail usually corresponds to diffusion-controlled processes or interfacial electrode polarization: therefore, ion migration might combine with electronic hopping in the Zinc framework.

# CONDUCTION MECHANISM DISCUSSION

The σac increases with frequency due to the Correlated Barrier Hopping (CBH) model or the Quantum Mechanical Tunnelling (QMT) model. At low frequencies, charge carriers must travel long distances, encountering higher resistance at grain boundaries. At higher frequencies, carriers have to hop between localized states over shorter distances (intra-grain), which greatly reduces the effective resistance and makes the conductivity increase. The difference observed across the three complexes is probably due to the varying electronic structures of the metal centers: $d^9$ for Cu, $d^8$ for Ni, and $d^{10}$ for Zn. The absence of partially filled orbitals due to the d10 configuration of Zn (II) usually undermines electronic hopping compared to the transition metal centers with unpaired electrons (Cu and Ni). The AC conductivity studies clearly show that the ($M_2$(DPBD)) complexes are semiconducting materials. The charge transport properties of the ($Cu_2$(DPBD)) complex are most efficient since this structure has lower bulk resistance and higher maximum σac. Although the ($Zn_2$(DPBD)) complex exhibits a less conductive configuration, its diffusion-related impedance profile is rather distinct, which may be of interest for electrochemical sensing or ion-transport applications.

***Electrochemical Impedance Spectroscopy (EIS) Analysis for ($Cu_2$(DPBD)):*** Electrochemical Impedance Spectroscopy (EIS) of the (Cu2(DPBD)) complex was conducted at different temperatures (25 °C, 35 °C, 45 °C, and 55 °C) in order to characterize its charge transport behavior. The Nyquist plots (-Z′ vs. Z′) of the obtained curves show a single semi-circular arc at each temperature, which indicates the parallel coupling of bulk resistance ($R_b$) and capacitance (C). The diameter of the semicircular arc represents the Charge Transfer Resistance ($R_{ct}$) or Bulk Resistance ($R_b$) of the complex. Increased temperature from 25 °C (green) to 55 °C (dark blue) significantly and systematically reduces the diameter of the semicircles. Rb figures (at Z"=0 intercepts); 25 °C 80,000 Ω; 35 °C 48,000 Ω; 45 °C 33,000 Ω; and 55 °C 22,000 Ω.

***Conductivity Enhancement:*** The reduction in resistance with increasing temperature indicates that the ($Cu_2$(DPBD)) complex exhibits semiconducting behavior. The total conductivity (σ) can be calculated using the formula:

$$\sigma = \frac{L}{R_b . A}$$

where L is the thickness and A is the cross-sectional area of the pellet/sample. The decreasing $R_b$ directly correlates to a thermally activated increase in conductivity.

***Thermally Activated Charge Transport:*** We see decreased impedance in a consistent, stepwise manner with increasing temperature, demonstrating that the charge carriers (in this case, either ions or electrons) have sufficient kinetic energy to jump over the activation energy barrier. This is common in coordination polymers or molecular complexes where charge transport is governed by a hopping mechanism.

***Equivalent Circuit Modelling:*** The plots can be fitted via an $R_s$ ($R_{ct}$.CPE) equivalent circuit having: $R_s$ is Ohmic resistance (intercept at the high-frequency/left side of the x-axis), $R_{ct}$ is charge transfer resistance (diameter of the arc), and CPE is constant phase element, which represents the non-ideal capacitive behavior of the complex due to surface roughness or inhomogeneous distribution of charge centers.

***Arrhenius Behavior:*** To further quantify this behavior, a plot of lnσ vs. 1000/T (Arrhenius Plot) can be generated. The linear relationship would allow for the calculation of the Activation

Energy ($E_a$) using the Arrhenius equation: $\sigma = e^{-E_a}/k_bT$

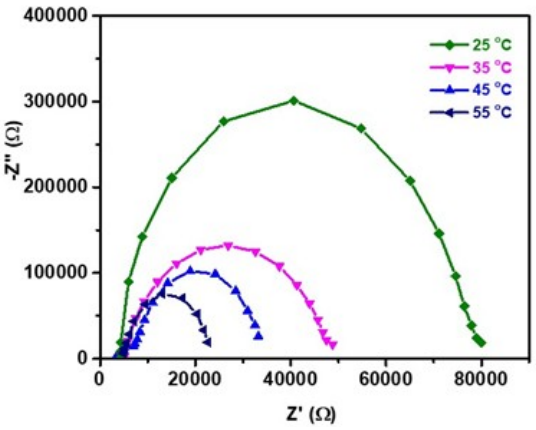


**Figure 6. Temperature-dependent Nyquist plots (-Z'' vs. Z') for the ($Cu_2$(DPBD)) complex recorded at 25 °C, 35°C, 45 °C, and 55 °C. The systematic reduction in the semicircular arc diameter with increasing temperature illustrates the decrease in bulk resistance ($R_b$), signifying the thermally activated charge transport and semiconducting nature of the bimetallic framework**

Decreasing the semicircle diameter drastically from 25 °C to 55 °C indicates a low activation energy and therefore may favor the feasibility of the ($Cu_2$(DPBD)) complex toward temperature-sensitive electronic or sensor applications. Last but by no means least, the temperature-dependent Nyquist plots prove that the ($Cu_2$(DPBD)) complex is a semiconductor. The bulk resistance dropped dramatically from 80 kΩ at room temperature to 22 kΩ at 55 °C, which shows the effective thermal activation of charge carriers in this framework of DPBD.

# CONCLUSION

Herein we have synthesized and demonstrated a series of binuclear ($M_2$(DPBD)$(OAc)_2$) complexes. TGA confirmed structural integrity and stoichiometry of metal-ligand framework and shows high thermal stability up to 450 °C. It demonstrated a significant solvatochromic shift and the generation of narrow UV-blue emission bands through the spectroscopic activity in metal coordination which serves to modulate the electronic environment of the DPBD ligand. The magnetic investigations revealed that the magnetic anisotropy and saturation levels depend on the metal center (Cu or Ni) adopted, with Nickel complex being found to have a higher magnetic performance. Electrically, the complex has the typical semi-conductivity under Jonscher's Power Law. The high-frequency AC conductivity and the dynamic impedance profiles of the Copper and Zinc analogs, especially at higher frequencies, indicate that the corresponding materials exhibit effective charge-carrier mobility. Collectively, its tunable optical capabilities, reliable thermal stability, and semiconductor-like transport modes make these bimetallic complexes attractive candidates as practical raw materials toward the next generation molecular electronics and functional magnetic materials.

# REFERENCES

1. Desiraju, G. R., Vittal, J. J. and A. Ramanan, *Crystal Engineering: A Textbook*, World Scientific, Singapore, 2011, pp. 131–153. (Foundations of coordination networks).
2. Batten, S. R., Neville, S. M. and D. R. Turner, *Coordination Polymers: Design, Analysis and Application*, Royal Society of Chemistry, London, **2009**, pp. 1–18.
3. Wu, H. C., Thanasekaran, P., Tsai, C. H., Wu, J. Y., Huang, S. M., Wen, Y. S. and Lu, K. L. 2006. "Supramolecular Isomerism in Coordination Polymers: Synthesis and Characterization of Bimetallic Frameworks," *Inorg. Chem.*, *45*, 295–303.
4. Yoshida, N., Ichikawa, K. and Shiro, M. 2000. "Excited-State Intramolecular Proton Transfer in 2,5-bis(pyridin-2-yl)benzene-1,4-diol and its Suppression upon Metal Coordination," *J. Chem. Soc., Perkin Trans. 2*, , 17–26. (Specific to the $DPBD$ ligand).
5. Massue, J., Ni, J. S., Jogani, S. and Ulrich, G. 2024. "ESIPT-active transition metal complexes: Coordination-induced fluorescence enhancement and solvatochromic tuning," *Dyes Pigm.*, *221*, 111842.
6. Jonscher, A. K. 1977. "The 'Universal' Dielectric Response," *Nature*, *267*, 673–679. (Foundational reference for the Power Law).
7. Jonscher, A. K. 1992. "The Universal Dielectric Response and its Physical Significance," *IEEE Trans. Electr. Insul.*, *27*, 407–423.
8. Paul, P. C., H. Pyngrope, and J. Chetia, "Luminescence of ESIPT-capable Zinc(II) Complexes: Exploring the Impact of Coordination on Proton-Donating Moieties," *J. Fluoresc.*, **2025**, *35*, 102–115.
9. Zhou, W., Fan, R. Q., Wang, P. and Yang, Y. L. 2012. "Synthesis and Photophysical Properties of Bimetallic Schiff-base Complexes derived from Pyridine-2-yl Precursors," *Acta Cryst. E*, *68*, o2086.
10. Zhou, H. C., J. R. Long, and O. M. Yaghi, "Introduction to Metal–Organic Frameworks," *Chem. Rev.*, **2012**, *112*, 673–674.
11. Natarajan, S., Mahata, P. and Sarma, D. 2012. "The Relevance of Metal Organic Frameworks (MOFs) in Inorganic Materials Chemistry: Magnetism and Luminescence," *J. Chem. Sci.*, *124*, 339–353.
12. Zaworotko M. J. and Moulton, B. 2001. "From Molecules to Crystal Engineering: Supramolecular

Isomerism in Network Solids," *Chem. Rev.*, *101*, 1629–1658.

13. Krivopalov, V. P., Vorob'eva, S. and Ryadun, A. A. 2023. "Complexes on the Base of a Proton Transfer Capable Pyrimidine Derivative: How Coordination Switches Emission Mechanisms," *Inorg. Chem.*, *62*, 16, 6542–6555.
14. MacDonald, J. R. 1985. "Generalizations of Universal Dielectric Response and a Distribution-of-Activation-Energies Model for Conducting Systems," *J. Appl. Phys.*, *58*, 1971.
15. Anisimov A. A. and Ananyev, I. V. 2024. "Coordination-driven Molecular Switches based on ESIPT-active Pyridine-Phenol Ligands," *J. Photochem. Photobiol. A*, *459*, 116091.

*******